BJP British Journal of Pharmacology

DOI:10.1111/bph.12480
www.brjpharmacol.org

RESEARCH PAPER

Differential interactions of antiretroviral agents with LXR, ER and GR nuclear receptors: potential contributing factors to adverse events

J Svärd[1]*, F Blanco[2], D Nevin[2], D Fayne[2], F Mulcahy[3], M Hennessy[1†] and J P Spiers[1†]

[1]*Department of Pharmacology and Therapeutics, Trinity College, Dublin, Ireland,* [2]*Molecular Design Group, School of Biochemistry and Immunology, Trinity Biomedical Sciences Institute, Trinity College, Dublin, Ireland, and* [3]*Department of Genitourinary Medicine and Infectious Disease, St James's Hospital, Dublin, Ireland*

Correspondence
Dr J P Spiers, Department of Pharmacology and Therapeutics, Trinity College Dublin, Trinity Centre for Health Sciences, St James's Hospital, Dublin 8, Ireland. E-mail: paul.spiers@tcd.ie

*Current address: Department of Medicine Huddinge, Karolinska Institutet, Stockholm, Sweden

†Joint authorship.

Keywords
antiretroviral drug; efavirenz; HIV protease inhibitor; nuclear receptor; liver X receptor; oestrogen receptor; glucocorticoid receptor; molecular modelling; ligand-binding domain; TR-FRET co-activator assay; luciferase reporter assay

Received
18 February 2013
Revised
30 September 2013
Accepted
15 October 2013

BACKGROUND AND PURPOSE

Antiretroviral (ARV) drugs activate pregnane X receptors and constitutive androstane receptors, increasing the risk of drug interactions due to altered drug metabolism and disposition. The closely related liver X receptors (LXRα/β), oestrogen receptors (ERα/β) and glucocorticoid receptor (GR) regulate many endogenous processes such as lipid/cholesterol homeostasis, cellular differentiation and inflammation. However, ARV drug activation of these nuclear receptors has not been thoroughly investigated.

EXPERIMENTAL APPROACH

The ability of an ARV drug library to activate LXRα/β, ERα/β and GR was assessed using a combined *in silico* and *in vitro* approach encompassing computational docking and molecular descriptor filtering, cell-free time-resolved fluorescence resonance energy transfer co-activator assays to assess direct binding to ligand-binding domains (LBDs), cell-based reporter assays and target gene expression.

KEY RESULTS

Direct LBD interactions with LXRα and/or LXRβ were predicted *in silico* and confirmed *in vitro* for darunavir, efavirenz, flavopiridol, maraviroc and tipranavir. Likewise, efavirenz was also predicted and confirmed as a ligand of ERα-LBD. Interestingly, atazanavir and ritonavir also activated LXRα/β in reporter assays, while tipranavir enhanced transcriptional activity of ERα. Effects on ER and LXR target gene expression were confirmed for efavirenz and tipranavir.

CONCLUSIONS AND IMPLICATIONS

There was good agreement between *in silico* predictions and *in vitro* results. However, some nuclear receptor interactions identified *in vitro* were probably due to allosteric effects or nuclear receptor cross-talk, rather than direct LBD binding. This study indicates that some of the adverse effects associated with ARV use may be mediated through 'off-target' effects involving nuclear receptor activation.

Abbreviations

11β-HSD1, hydroxysteroid 11-β dehydrogenase-1; ART, antiretroviral therapy; ARV, antiretroviral; ER, oestrogen receptor; GGPP, geranylgeranyl pyrophosphate; GR, glucocorticoid receptor; LBD, ligand binding domain; LXR, liver X receptor; PGC1α, PPARγ co-activator 1α; PI, protease inhibitor; PXR, pregnane X receptor; ROC, receiver operating characteristic; SREBP-1, sterol regulatory element binding protein; TR-FRET, time-resolved fluorescence resonance energy transfer; TRAP220/DRIP205, thyroid hormone receptor-associated protein 220/vitamin D receptor-interacting protein 2

Introduction

Members of the nuclear receptor superfamily, such as liver X receptor (LXR), oestrogen receptor (ER), glucocorticoid receptor (GR) and pregnane X receptor (PXR), are intrinsically involved in critical, diverse processes like metabolism, inflammation and neuronal function (Dahlman-Wright *et al.*, 2006; Lu *et al.*, 2006; Krasowski *et al.*, 2011; receptor nomenclature follows Alexander *et al.*, 2013). Selectivity of ligand-dependent transcriptional activation is determined by the structure of the ligand binding domain (LBD), which is often highly conserved between nuclear receptor homologues (Ekins *et al.*, 2002). The LBDs also interact with numerous co-regulatory proteins. For example, the PPARγ co-activator 1α (PGC1α) and TRAP220/DRIP205 (thyroid hormone receptor-associated protein 220/vitamin D receptor-interacting protein 2) are established co-activators of LXR, ER and PPARs (Tcherepanova *et al.*, 2000; Vega *et al.*, 2000; Oberkofler *et al.*, 2003; Son and Lee, 2009). Upon agonist binding, the receptor undergoes a conformational change that releases the co-repressor, permitting co-activator recruitment and initiation of signalling, culminating in gene expression.

Antiretroviral therapy (ART) is associated with a spectrum of metabolic side effects, including lipid abnormalities, fat redistribution and glucose intolerance (Haugaard, 2006). At the cellular level, this is linked to altered expression of several genes associated with lipid and metabolic homeostasis. For instance, in adipose tissue from ART-treated HIV patients suffering from lipoatrophy, mRNA expression of hydroxysteroid 11-β dehydrogenase-1 (*11β-HSD1*), *PPARγ* and sterol regulatory element binding protein (*SREBP-1*) are reduced (Bastard *et al.*, 2002; Sutinen *et al.*, 2004; Kratz *et al.*, 2008). Interestingly, LXR, ER and GR are involved in transcriptional regulation of 11β-HSD1 (Stulnig *et al.*, 2002; Yang *et al.*, 2007; van den Driesche *et al.*, 2008), while LXR is also implicated in transcriptional regulation of *SREBP-1* and *PPARγ* (Repa *et al.*, 2000; Seo *et al.*, 2004). Therefore, LXR, ER and GR may mediate some of the 'off-target' effects associated with ART.

Direct supporting evidence of this is limited, as most studies use surrogate markers of nuclear receptor activation, sometimes with conflicting results. For example, ritonavir increases *SREBP-1* (LXR target gene) expression in macrophages (Zhou *et al.*, 2005) and adipocytes (Nguyen *et al.*, 2000), while others found that ritonavir-induced dyslipidaemia is associated with nuclear accumulation of SREBP-1, independent of changes in SREBP-1 mRNA expression (Riddle *et al.*, 2001). Effects may be drug-specific, as indinavir decreases protein levels of SREBP-1 in adipocytes (Caron *et al.*, 2001) and mRNA expression in fat from HIV patients treated with indinavir or nelfinavir in combination with stavudine/lamivudine compared with healthy controls (Bastard *et al.*, 2002). With regard to the ER, female LDL-null mice exposed to ritonavir or amprenavir develop fewer atherosclerotic lesions compared with males, an effect that is obliterated by homozygous knockout of ERα (Allred *et al.*, 2006). Due to intricate cross-regulation, it is difficult to attribute changes in gene expression to specific nuclear receptors. In order to characterize interactions between antiretroviral compounds and LXR, ER or GR, experiments assessing direct nuclear receptor activation are required.

Therefore, the aims of the present study were to (i) define structural docking models for LXRα/β, ERα/β and GR, (ii) predict the ability of a library of antiretroviral drugs to act as ligands using *in silico* modelling; (iii) assess direct binding to LBDs using cell-free time-resolved fluorescence resonance energy transfer (TR-FRET) co-activator assays, (iv) assess nuclear receptor activation using cell-based luciferase reporter assays and (v) confirm effects on target gene expression.

Methods

Establishment of nuclear receptor LBD docking models

Ligand docking protocols were established for LXRα (NR1H3), LXRβ (NR1H2), ERα (NR3A1), ERβ (NR3A2) and GR (NR3C1), based upon structures documented in the Research Collaboration for Structural Collaboration Protein Data Bank (http://www.rcsb.org; LXR 44 structure hits/33 citations, ER 123 structure hits/58 citations and GR 73 structure hits/32 citations). In the selection of crystal structures for the analysis, resolution, R-value, R-free and EC_{50} of the associated ligand were considered (Table 1). Structures of the receptors co-crystallized with ligands were preprocessed using Molecular Operating Environment software (MOE version 2010.10; Chemical Computing Group, Montreal, Canada). The positions of hydrogen atoms and partial charges were calculated and a molecular force field minimization step performed using AMBER99 (Assisted Model Building with Energy Refinement) implemented in MOE. Co-activators and secondary water molecules were removed and the shape and features of the LBDs explored using MOE applications. The five preprocessed receptors were prepared for docking analysis with Fast Rigid Exhaustive Docking software (FRED version 2.2.5; OpenEye Scientific Software, Santa Fe, NM, USA; http://www.eyesopen.com) using the *fred_receptor* application. Shape-based filters were used to eliminate compounds in the database that were not complementary to the binding site of interest. Rigid rotation and translation of the molecules was used to optimize ligand poses from the exhaustive docking.

Table 1

Details of nuclear receptor LBD X-ray structures selected for *in silico* analysis

Receptor	PDB code	Resolution (nm)	R-value	R-free	Ligand	IC_{50}/EC_{50} (nM)[a]
LXRα	3IPQ	0.200	0.201	0.234	GW3965	80.0–660.0
LXRβ	1PQ6	0.240	0.209	0.262	GW3965	20.0–410.0
ERα	1XPC	0.160	0.184	0.251	AIT	0.04–1.3
ERβ	3OLL	0.150	0.177	0.208	E2	0.1–30.0
GR	1M2Z	0.250	0.267	0.267	DEXA	0.2–7.2

All structures correspond to human sequences.
PDB, Protein Data Bank (http://www.rscb.org); GW3965, synthetic LXR ligand; AIT, (2*S*,3*R*)-3-(4-hydroxyphenyl)-2-[4-[(2*R*)-2-pyrrolidin-1-ylpropoxy]phenyl]-2,3-dihydro-1,4-benzoxathiin-6-ol (compound 19), E2, 17β-oestradiol, DEXA, dexamethasone.
[a]Ligand affinity data from BindingDB (http://www.bindingdb.org).

Table 2

Docking validation test data

Receptor	N actives	N decoys	D actives	D decoys	ROC AUC
LXRα	70	2564	70	504	0.754
LXRβ	70	2564	70	504	0.829
ERα	67	2570	67	2351	0.907
ERβ	67	2570	67	2351	0.843
GR	78	2947	78	2583	0.595

N, number of input molecules; D, number of molecules passing docking validation; ROC AUC, receiver operating characteristic area under curve.

Following extensive in-house scoring function evaluation against multiple nuclear receptors, the *Chemgauss3* scoring function (FRED) was used to score the optimized poses and represent an estimation of the binding affinity.

Validation of the nuclear receptor LBD docking models

Validation of the modelling was assessed by the ability of the model to retrieve known active compounds from a database containing both actives and decoys (known inactive compounds). For ER and GR receptors, sets of actives/decoys were downloaded from http://www.dud.docking.org (Huang *et al.*, 2006), while a set of actives/decoys was built for the LXR receptors using parameters recommended on the same website, with ~36 decoys for each active (Table 2). The decoys selected had similar physicochemical and structural properties as the actives, but dissimilar topology. The distribution of molecular descriptors for the sets of active ligands is presented in Table 3. All molecules were preprocessed with MOE to add hydrogen atoms and partial charges, while energy minimization was performed using MMFF94x (Merck Molecular Force Field). OMEGA software (OMEGA version 2.4.3, OpenEye Scientific Software) (Hawkins *et al.*, 2010) was utilized with default parameters for conformational searches in order to generate 50 conformers for each active/decoy. Receiver operating characteristic (ROC) curves were constructed to assess the ability of each model to distinguish known actives from decoys.

Evaluation of antiretroviral (ARV) compounds as nuclear receptor ligands

A library of 26 ARV compounds (Table 4) was evaluated for binding to LXRα, LXRβ, ERα, ERβ and GR using FRED. Each compound was preprocessed in MOE, and energy minimization was performed as described above. Conformers (50 per compound) were generated using OMEGA software and used for docking. Docking scores were calculated using the *Chemgauss3* scoring function in FRED. Results from the docking analysis were filtered based upon molecular descriptors for known ligands of each nuclear receptor: number of hydrogen donors, hydrogen acceptors, nitrogen atoms, oxygen atoms, rotatable bonds, hydrophobic bonds, rings, logP and molecular weight (Table 3). Compounds falling outside the descriptor ranges, even those passing the docking test, were not considered as potential ligands.

Fluorescence co-activator assays

TR-FRET co-activator assays (LanthaScreen, Invitrogen, Paisley, UK) were utilized to assess binding of selected antiretroviral compounds to the ligand-binding domain of the LXRα, LXRβ and ERα nuclear receptors. Compounds were selected on the basis of (i) *in silico* modelling (LXRα/β ligands: darunavir, tipranavir, efavirenz, maraviroc, TAK-779, flavopiridol; ERα ligands: efavirenz, flavopiridol), (ii) being known PXR inducers (fosamprenavir, lopinavir, nelfinavir), (iii) lipodystrophy association (ritonavir), (iv) favourable lipid

Table 3

Molecular descriptors of typical known ligands for LXRα, LXRβ, ERα, ERβ and GR

Molecular descriptor	LXRα	LXRβ	ERα	ERβ	GR
Number of hydrogen donors	<3	<3	<4	<4	<3
Number of hydrogen acceptors	<6	<6	<6	<6	<5
Number of hydrophobic atoms	16–42	16–42	10–25	10–25	15–30
Number of nitrogens	<5	<5	<2	<2	<2
Number of oxygens	<7	<7	<6	<6	<5
Number of rotatable bonds	<18	<18	<6	<6	<6
Number of rings	<6	<6	<5	<5	<5
LogP	<12	<12	<6	<6	<8
Molar weight (g mol^{-1})	300–700	300–700	200–375	200–375	250–500

Table 4

ARV compounds included in the molecular modelling analysis

ARV drug	Abbreviation	Class	Molecular formula	Molar weight (g mol^{-1})
Atazanavir	ATV	PI	$C_{38}H_{52}N_6O_7$	704.87
Darunavir	DRV	PI	$C_{27}H_{37}N_3O_7S$	546.66
Fosamprenavir	FOS	PI	$C_{25}H_{36}N_3O_9PS$	585.61
Indinavir	IDV	PI	$C_{36}H_{47}N_5O_4$	613.79
Lopinavir	LPV	PI	$C_{37}H_{48}N_4O_5$	628.81
Nelfinavir	NFV	PI	$C_{32}H_{45}N_3O_4S$	567.79
Ritonavir	RTV	PI	$C_{37}H_{48}N_6O_5S_2$	720.95
Saquinavir	SQV	PI	$C_{38}H_{50}N_6O_5$	670.85
Tipranavir	TPV	PI	$C_{31}H_{33}F_3N_2O_5S$	602.67
Abacavir	ABC	NRTI	$C_{14}H_{18}N_6O$	286.34
Didanosine	ddI	NRTI	$C_{10}H_{12}N_4O_3$	236.23
Emtricitabine	FTC	NRTI	$C_8H_{10}FN_3O_3S$	247.25
Lamivudine	3TC	NRTI	$C_8H_{11}N_3O_3S$	229.26
Stavudine	d4T	NRTI	$C_{10}H_{12}N_2O_4$	224.22
Tenofovir	TFV	NRTI	$C_9H_{14}N_5O_4P$	287.22
Zalcitabine	ddC	NRTI	$C_9H_{13}N_3O_3$	211.22
Zidovudine	AZT	NRTI	$C_{10}H_{13}N_5O_4$	267.25
Efavirenz	EFV	NNRTI	$C_{14}H_9ClF_3NO_2$	315.68
Etravirine	TMC125	NNRTI	$C_{20}H_{15}BrN_6O$	435.29
Nevirapine	NVP	NNRTI	$C_{15}H_{14}N_4O$	266.30
Maraviroc	MVC	CCR5 antagonist	$C_{29}H_{41}F_2N_5O$	513.68
TAK-779	–	CCR5 antagonist (investigational)	$C_{33}O_2N_2H_{38}$	495.69
Bicyclam JM-2987	Hydrobromide salt of AMD-3100	CXCR4 antagonist (investigational)	$C_{30}H_{70}Br_8N_8O_4$	506.83
Raltegravir	MK-0518	Integrase inhibitor	$C_{20}H_{20}FKN_6O_5$	444.42
118-D-24	–	Integrase inhibitor (investigational)	$C_{11}H_9N_3O_4$	247.2
Flavopiridol	FLAV	Cdk inhibitor (investigational)	$C_{21}H_{20}O_5NCl$	402.85

PI, protease inhibitor; NRTI, nucleoside reverse transcriptase inhibitor; NNRTI, non-nucleoside reverse transcriptase inhibitor, Cdk, cyclin-dependent kinase.

profile (atazanavir) or (v) being modulators of SREBP-1c mRNA and protein expression (indinavir). Assays were performed according to the manufacturer's instructions, using PGC1α, TRAP220/DRIP205 or D22 (Stafslien *et al.*, 2007) as co-activators. Assays were validated using the established LXRα/β and ERα agonists T0901317 and 17β-oestradiol. Initial experiments were undertaken to detect effects at 100 μM, followed by serial dilutions in DMSO (46 nM to 100 μM) for any initial hits. All test concentrations were run in triplicate in 384-well plates, along with a vehicle control, a positive control (20 μM T0901317 or 1 μM 17β-oestradiol) and a 'no LBD' control. To test if compounds demonstrated LXRα antagonistic properties (based on the initial screen), dose–response curve in the presence of T0901317 (EC_{80} = 1.5 μM) was also assessed; GGPP (1 μM) was used as a positive control. All assays were incubated for 2 h at room temperature in the dark, and FRET was quantified by measurement of the emission ratio at 520/495 nm (BMG PheraStar microplate reader, BMG Labtech, Offenburg, Germany).

Reporter assays: plasmids

Professor DJ Mangelsdorf (University of Texas Southwestern Medical Center, TX, USA) provided the human pCMX-LXRα and pCMX-LXRβ plasmids. The 3xhLXRE-luc plasmid was constructed from the human *ABCA1* promoter, including three repeats of the minimal DR4 motif (Wong *et al.*, 2007), and was donated by Professor AJ Brown (University of New South Wales, Australia). Human pSG5-ERα and pSG5-ERβ were gifts from Professor Jan-Åke Gustafsson (Karolinska Institutet, Sweden). Human 3xERE-TATA-luc, containing three copies of the human vitellogenin gene *ERE* (Hall and McDonnell, 1999), was constructed by Professor DP McDonnell (Duke University Medical School, NC, USA) and obtained through Addgene (plasmid 11354) (Cambridge, MA, USA). Human pCMV6-GR and GR-luc were purchased from Origene (Rockville, MD, USA) and Panomics (Fremont, CA, USA), respectively. pRL-TK (expressing *Renilla* luciferase) was obtained from Promega (Madison, WI, USA) and used as an internal standard.

HepG2 cell culture and transfection

HepG2 cells [European Collection of Cell Cultures (ECACC), Salisbury, UK] were cultured in Eagle's minimum essential medium, supplemented with 10% fetal bovine serum (FBS), 2 mM L-glutamine, 100 units penicillin, and 0.1 mg ml^{-1} streptomycin (Sigma-Aldrich). Prior to transient transfection, cells were seeded onto 24-well plates (40 000 cells/well) and allowed to attach overnight. Cells were transfected with the LXR and GR reporter systems consisting of the nuclear receptor expression plasmid, response element–luciferase construct and internal standard (LXR: 5 ng pCMX-LXRα or pCMX-LXRβ + 400 ng 3xhLXRE-luc + 50 ng pRL-TK; GR: 5 ng pCMV6-GR + 400 ng GR-luc + 50 ng pRL-TK), using Lipofectamine LTX (Invitrogen) according to manufacturer's instructions. Transfections were allowed to proceed for 8–9 h in serum- and antibiotic-free medium prior to drug exposure. For the ER experiments, cells were cultured in phenol red-free minimum essential medium (Gibco/Invitrogen, Paisley, UK) supplemented with 10% charcoal-stripped FBS, 2 mM L-glutamine and antibiotics for 32 h prior to transfection. Transfection (15 h) was performed in phenol red-, serum- and antibiotic-free medium using Lipofectamine LTX and 500 ng ER plasmid (pSG5-ERα or pSG5-ERβ), 1 μg 3xERE-TATA-luc and 200 ng pRL-TK.

Drug exposure and assessment of luciferase activity

Transfected cells were washed with phosphate buffered saline (Sigma-Aldrich), and the medium was replaced with phenol red-free minimum essential medium (Gibco/Invitrogen) supplemented with glutamine and antibiotics, containing either 10% charcoal-stripped FBS (ERα, ERβ, GR) or 5% fetal bovine lipoprotein-deficient serum (FB-LPDS; Intracel, Frederick, MD, USA). Cells were exposed to selected antiretroviral agents (as used in the TR-FRET assay) at a concentration of 10 μM, with the exception of nelfinavir (1 μM) and flavopiridol (100 nM), due to cytotoxicity. Positive controls for LXR (10 μM T0901317), ER (100 nM 17β-oestradiol, E2) and GR (1 μM dexamethasone) were included, along with vehicle control (0.1% v/v DMSO). Following drug exposure (24 h for LXRs and GR, 30 h for ERs), cells were harvested and lysed, and firefly and *Renilla* luciferase activity were measured using a Dual-Luciferase Reporter Assay System (Promega) and a luminometer (Thermo Fisher Scientific, Dublin, Ireland).

Effects on gene expression

SH-SY5Y expressing cells (ABCA1) were obtained from ECACC and cultured in Dulbecco's modified Eagle's medium/nutrient mixture F-12 Ham supplemented with 2 mM L-glutamine, antibiotics, 1% non-essential amino acids and 10% FBS. *PGR* expression was assessed in MCF-7 cells (Dr Steven Gray, Trinity College Dublin) and cultured in minimum essential medium with 2 mM L-glutamine, antibiotics and 10% FBS. Cells were seeded in six-well plates (SH-SY5Y: 3 x 10^5 cells per well; MCF-7: 5 x 10^5 cells per well) and washed the following day prior to drug exposure (24 h) in complete phenol red-free medium with 5% FB-LPDS (SH-SY5Y) or 10% FBS (MCF-7). ARVs selected on the basis of reporter data were assessed in SH-SY5Y or MCF-7 as appropriate, at concentrations of 10 μM or 100 nM (flavopiridol). Controls included DMSO (0.1% v/v), T0901317 (10 μM) and 17β-oestradiol (100 nM).

Total RNA was isolated using TRIsure (Bioline, UK), and treated with DNase I prior to reverse transcription using random hexamers and M-MuLV reverse transcriptase (RevertAid Reverse Transcriptase, Thermo Scientific). The expression of *ABCA1* (NM_005502.3), *PGR* (progesterone receptor; NM_000926.4) and *GAPDH* (NM_002026) was analysed by comparative quantitation using QuantiTect primer assays (Qiagen, Crawley, UK) and a QuantiTect SYBR Green RT-PCR kit on a Mx3000p real-time PCR system (Agilent, Cork, Ireland). Relative mRNA expression of the target genes was calculated using MxPro software based upon the $2^{-[\Delta\Delta Ct]}$ method (Pfaffl, 2001), following normalization to GAPDH.

Data analysis

Data from the TR-FRET co-activator assays (n = 6) were baseline subtracted, and concentration–response curves were constructed for all agonists/antagonists and fitted using a sigmoidal dose–response curve (variable slope). Maximum response ratios (%, n = 3) were calculated in comparison

with positive controls for agonist assays – T0901317 (20 μM), 17β-oestradiol (1 μM), dexamethasone (1 μM) or GGPP (1 μM) – and in comparison to T0901317 (1.5 μM) for LXRα antagonist assays. One-way ANOVA followed by Dunnett's *post hoc* test was used to assess change from baseline in dose–response curves. EC_{50} or IC_{50} values are expressed as mean ± SEM.

Luciferase reporter assay data (n = 5) are expressed as the ratio of firefly luciferase activity to *Renilla* luciferase activity. In real-time PCR experiments (n = 5), expression of *PGR* and *ABCA1* was normalized to *GAPDH*. Results from both reporter assays and real-time PCR experiments are presented relative to DMSO (mean ± SEM). For one-way ANOVA with Dunnett's *post hoc* analysis, data were first transformed (log_{10}). Statistical analyses were performed using GraphPad Prism version 5, with $P \leq 0.05$ indicating significance.

Materials

Abacavir, atazanavir, flavopiridol, maraviroc, TAK-779 and tipranavir were obtained through the AIDS Research and Reference Reagent Program, Division of AIDS, National Institute of Allergy and Infectious Diseases, NIH (Bethesda, MD, USA). Tibotec (Titusville, NJ, USA) provided darunavir, via the same program. Fosamprenavir, lopinavir and nelfinavir were gifts from GlaxoSmithKline (Hertfordshire, UK), Abbott (Abbott Park, IL, USA) and Pfizer (Groton, CT, USA), respectively. Efavirenz was purchased from LGM Pharmaceuticals (Boca Raton, FL, USA), while indinavir and ritonavir were acquired from USP Reference Standards (Rockville, MD, USA). T0901317, 17β-oestradiol, dexamethasone and geranylgeranyl pyrophosphate (GGPP) were purchased from Sigma-Aldrich (Wicklow, Ireland). All drug stocks were dissolved in DMSO, except TAK-779, which was reconstituted in water; 17β-oestradiol and dexamethasone, which were dissolved in ethanol; and GGPP, which was supplied in a solution of methanol:NH_4OH (7:3).

Results

Docking validation and ARV evaluation

A comparison of the nuclear receptor ligand-binding pockets shows smaller sizes for ER and GR, compared with that of LXR, which is more extended. The three receptor types display predominantly hydrophobic ligand-binding pockets, with a few specific hydrophilic areas involved in hydrogen bond interactions (Figure 1). The validation of the docking models as measured by ROC area under curve coefficients classified ERα (0.907) as excellent, LXRα (0.754) as fair, and LXRβ (0.829) and ERβ (0.843) as good, while the ROC curve for GR (0.595) is close to a diagonal line (equivalent to random hits), and hence a poor quality model. Previous work demonstrated that a ligand-based design approach is more appropriate to GR than docking (Onnis *et al.*, 2010). Consequently, scoring results for the latter must be considered statistically less reliable. ARV docking scores and results from filtering by molecular descriptor ranges for each receptor are presented in Tables 5–9.

The ARV compounds that passed the LXRα docking test and were compatible with the molecular descriptors were (in order of best *Chemgauss3* docking score) darunavir (–101.01), maraviroc (–98.35), flavopiridol (–88.84), efavirenz (–86.71) and, with weaker scores but still ranked high enough to be considered potentially active, TAK-779 (–62.81) and tipranavir (–61.12). For comparison, 95% of the known actives for LXRα scored below –80.00. Potential LXRβ ligands identified were TAK-779 (–107.86), maraviroc (–99.84), flavopiridol (–89.65) and, with weaker scores but still considered to be active, were efavirenz (–84.91), tipranavir (–81.21) and darunavir (–74.39), for which 95% of known actives scored below –88.00. Only efavirenz passed the ERα and ERβ *in silico* screenings, scoring –72.73 and –64.20, respectively. This was just outside the known actives range (<–75.00 for ERα and <–70.00 for ERβ) but still ranked well enough to be considered a potential ER binder. Using the GR docking model, both flavopiridol (–90.85) and efavirenz (–89.75) were identified as potential ligands (both within the known actives *Chemgauss3* score range of below –64.00). The most common molecular descriptor leading to exclusion of compounds from the list of potential candidates, despite passing the docking test, was number of hydrophobic atoms (too few) for LXRα and LXRβ. This, in addition to number of nitrogens (too many), was a common reason for exclusion in the ERα, ERβ and GR analyses. The molecules that failed the docking tests of all five receptors were usually too large and had too few rotatable bonds.

Assessment of direct receptor LBD interactions: fluorescence co-activator assays

To assess direct binding of ARV drugs (predicted as potential ligands *in silico*) to the LBDs of LXRα, LXRβ and ERα, TR-FRET co-activator assays were utilized. Initial screening experiments with the drugs at a concentration of 100 μM were carried out using PGC1α and TRAP220/DRIP205 as co-activators for LXRα and ERα. In LXRα experiments, recruitment of PGC1α yielded a larger increase in fluorescence signal than TRAP220/DRIP205 and was subsequently used in the dose–response experiments with potential ligands predicted from the *in silico* modelling. T0901317 (EC_{50} = 214 nM) was used as a positive control to verify assay functionality. The maximum response ratios to the response in the presence of 20 μM T0901317 were as follows: 28.9% for maraviroc, 11.9% for darunavir and 10.4% for tipranavir at the highest concentration tested (100 μM), all of which were significantly different ($P < 0.05$) to baseline (DMSO). Based upon the dose–response data (Figure 2A), maraviroc and darunavir had EC_{50} values of 14.5 μM and 19.1 μM, respectively, while tipranavir EC_{50} could not be determined at the concentrations tested. Initial screening of the ARV drugs in LXRα binding assays indicated that efavirenz, TAK-779 and flavopiridol reduced TRAP220/DRIP205 recruitment. To confirm this, their effects were assessed in antagonist assays utilizing T0901317 (1.5 μM) as the agonist. At the highest concentration studied (100 μM), efavirenz and TAK-779 inhibited the response by approximately 60% ($P < 0.05$; Figure 2B), with IC_{50} values of 39.2 μM and 41.7 μM, respectively. Flavopiridol showed a trend towards reduced TRAP220/DRIP205 recruitment by LXRα; however, the dose–response curve did not converge, and the reduction at the highest concentration tested was not significant (Figure 2B). GGPP (LXR antagonist) inhibited the response by 18% at

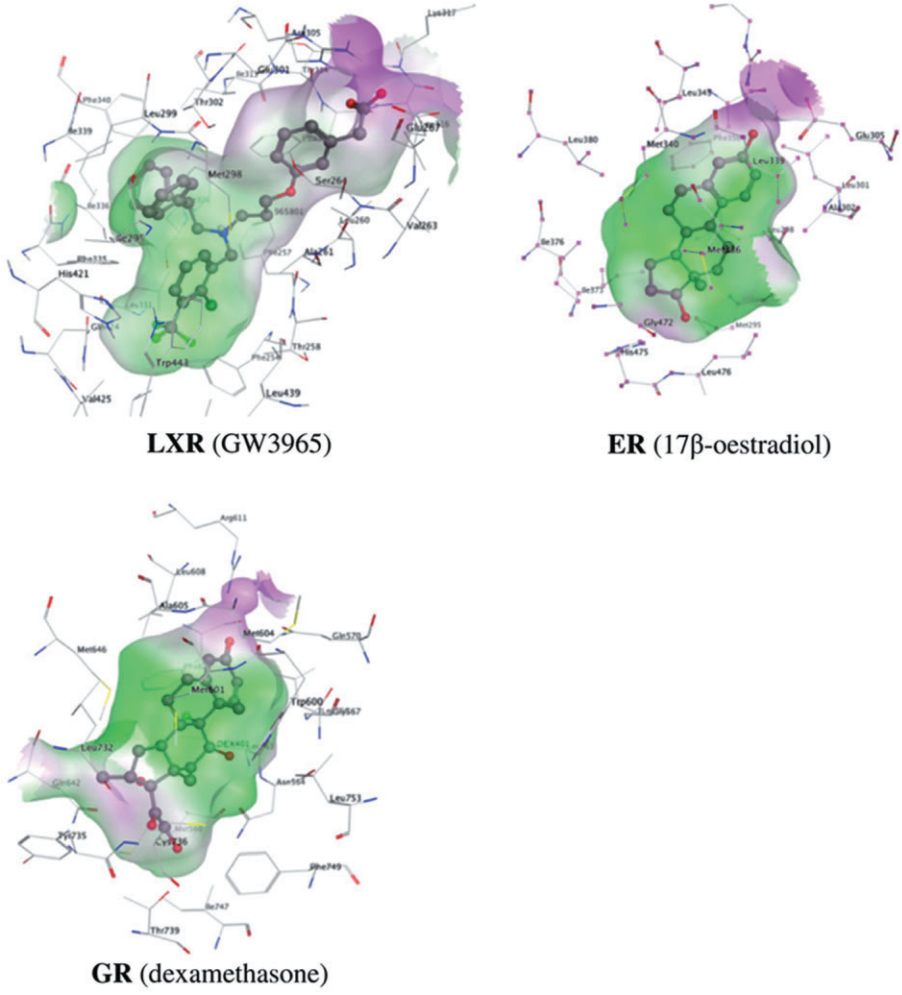

Figure 1

Ligand-binding pockets of LXR, ER and GR. Views of the three receptor families with prototypical ligands (in brackets) obtained using MOE software. Hydrophobic, neutral and hydrophilic regions are shown in green, white and violet respectively.

1 μM (highest concentration tested). As several ARV drugs were also predicted as ligands of LXRβ, TR-FRET co-activator assays were carried out with this nuclear receptor LBD. However, none of the ARV drugs tested in high-dose single concentrations affected D22 co-activator recruitment by LXRβ, while the IC_{50} of T0901317 was 304 nM. As efavirenz and flavopiridol functioned as antagonists in LXRβ reporter assays, additional TR-FRET experiments were carried out using the following co-repressors: SMRT ID1, SMRT ID2, NCoR ID1 and NCoR ID2. Data from these experiments indicated that neither of the drugs affected recruitment of the LXRβ co-repressors (data not shown).

In ERα TR-FRET assays, none of the ARVs tested altered either PGC1α or TRAP220/DRIP205 recruitment. The positive control, 17β-oestradiol, elicited robust recruitment of both PGC1α (IC_{50} = 0.7 nM) and TRAP220/DRIP205 (IC_{50} = 0.6 nM) to ERα.

Z′ factors were calculated for all TR-FRET experiments and ranged between 0.64–0.84, indicating that all assays were robust (1 indicates a theoretically ideal assay).

Reporter assays

The ability of ARV drugs to activate LXRα/β, ERα/β or GR in a cell-based system was assessed by *in vitro* luciferase reporter assays. All ARV drugs were used at 10 μM except nelfinavir (1 μM) and flavopiridol (100 nM). T0901317 (positive control, 10 μM) induced a 9.3 ± 0.9-fold change in LXRα transcriptional activity compared with vehicle control and a 2.8 ± 0.2-fold change of LXRβ transcriptional activity (P < 0.05). Atazanavir, darunavir and ritonavir increased LXRα transcriptional activity by 3.3-, 1.8- and 3.5-fold, respectively (Figure 3A). For LXRβ, the corresponding values were 3.1 ± 0.2 (atazanavir), 2.1 ± 0.2 (darunavir) and 2.4 ± 0.4 (ritonavir). In contrast, efavirenz reduced basal LXRα reporter activity by ~70% and basal LXRβ activity by ~90%. Furthermore, maraviroc and tipranavir increased LXRβ transcriptional activity by ~1.5-fold, while flavopiridol decreased it by ~70% compared to vehicle control (P < 0.05; Figure 3B).

Transcriptional activity of ERα was increased by efavirenz (P < 0.05; fold change 11.3 ± 2.2) and tipranavir (P < 0.05; fold

Table 5

LXRα docking score results

	LXRα										
Molecule	**S_{Dock}**	**N_{Dock}**	**a_don**	**a_acc**	**a_hyd**	**a_nN**	**a_nO**	**b_rotN**	**Rings**	**log P**	**Mw**
Actives range	*<–80.00*	*–*	*<3*	*<6*	*16–42*	*<5*	*<7*	*<18*	*<6*	*<12*	*300–700*
TMC125	–104.47	70.57	2	4	16	6	1	6	3	3.81	435.29
DRV	–101.01	68.23	3	6	24	3	7	13	4	2.15	546.66
MVC	–98.35	66.43	1	4	28	5	1	9	5	6.64	513.68
FLAV	–88.84	60.01	3	4	21	1	5	2	4	2.90	402.85
ABC	–88.58	59.84	3	4	10	6	1	4	4	0.41	286.34
RAL	–87.95	59.41	3	7	15	6	5	8	3	0.81	444.42
EFV	–86.71	58.57	1	1	17	1	2	3	3	4.10	315.68
118-D-24	–83.59	56.46	3	6	8	3	4	6	1	1.16	248.22
AZT	–78.76	53.20	2	6	7	5	4	4	2	–1.91	267.25
NVP	–78.45	52.99	1	3	12	4	1	1	4	1.90	266.30
IDV	–77.91	52.63	4	7	34	5	4	14	5	2.76	613.80
TFV	–75.36	50.90	4	7	5	5	4	5	2	–1.60	287.22
ddI	–73.74	49.81	2	5	5	4	3	2	3	0.13	236.23
ddC	–72.51	48.98	2	4	6	3	3	2	2	–0.50	211.22
FTC	–68.52	46.28	2	4	7	3	3	2	2	–0.52	247.25
NFV	–67.60	45.66	4	5	31	3	4	12	4	5.36	567.79
3TC	–67.16	45.37	2	4	6	3	3	2	2	–0.75	229.26
d4T	–63.50	42.89	2	4	7	2	4	2	2	–1.01	224.22
TAK-779	–62.81	42.43	1	2	32	2	2	7	5	6.45	495.69
TPV	–61.12	41.28	2	5	33	2	5	12	4	7.68	602.67
FOS	–59.82	40.41	5	8	24	3	9	15	3	1.50	585.61
JM2987	–40.54	27.38	3	3	27	8	0	4	3	0.92	506.83
LPV	–2.98	2.01	4	5	34	4	5	17	4	5.19	628.81
SQV	25.76	-17.40	5	7	34	6	5	16	5	3.31	670.85
ATV	F	-	5	7	34	6	7	22	3	4.74	704.87
RTV	F	-	4	6	36	6	5	22	4	5.00	720.96

Actives range for S_{Dock} indicates the limit above which 95% of the known actives scored. Dark grey indicates compound outside actives range of molecular descriptors

S_{Dock}, docking score using *Chemgauss3* scoring function (FRED software); N_{Dock}, S_{Dock} value normalized to best-scoring known active; a_don, number of hydrogen donors; a_acc, number of hydrogen acceptors; a_hyd, number of hydrophobic atoms; a_nN, number of nitrogens; a_nO, number of oxygens; b_rotN, number of rotatable bonds; rings, number of rings; mw, molar weight (g mol^{-1}); F, compound failed docking test (listed in no specific order). See Table 4 for drug name abbreviations.

change 5.5 ± 1.7; Figure 3C). None of the ARV drugs tested had an effect on ERβ (Figure 3D) or GR promoter activation (Figure 3E). A summary of results from *in silico* analysis, TR-FRET co-activator experiments and luciferase reporter assays is presented in Table 10.

Nuclear receptor target gene expression

T0901317 and 17β-oestradiol increased ($P < 0.05$) ABCA1 and PGR mRNA expression by approximately ninefold. Efavirenz and ritonavir reduced ($P < 0.05$) *ABCA1* expression in SH-SY5Y cells by 80% and 50%, respectively (Figure 4A). None of the other ARVs tested altered *ABCA1* expression. Exposure of MCF-7 cells to efavirenz and tipranavir increased *PGR* mRNA by 2.6 ± 0.3- and 4.7 ± 0.4-fold (Figure 4B).

Discussion

Activation of PXR and CAR by ARV drugs, mainly protease inhibitors (PIs), has been described previously (Gupta *et al.*, 2008; Svard *et al.*, 2010). However, investigations of ARV interactions with other nuclear receptors are largely limited to indirect markers such as target gene expression and to small numbers of study drugs. Considering the many adverse metabolic effects experienced by HIV patients undergoing

Table 6

LXRβ docking score results

			LXRβ								
Molecule	**S_{Dock}**	**N_{Dock}**	**a_don**	**a_acc**	**a_hyd**	**a_nN**	**a_nO**	**b_rotN**	**rings**	**log P**	**Mw**
Actives range	*<–88.00*		*<3*	*<6*	*16–42*	*<5*	*<7*	*<18*	*<6*	*<12*	*300–700*
TAK-779	–107.86	72.09	1	2	32	2	2	7	5	6.45	495.69
TMC125	–103.74	69.33	2	4	16	6	1	6	3	3.81	435.29
RAL	–101.32	67.71	3	7	15	6	5	8	3	0.81	444.42
MVC	–99.84	66.72	1	4	28	5	1	9	5	6.64	513.68
ABC	–90.52	60.49	3	4	10	6	1	4	4	0.41	286.34
FLAV	–89.65	59.91	3	4	21	1	5	2	4	2.90	402.85
EFV	–84.91	56.74	1	1	17	1	2	3	3	4.10	315.68
TFV	–83.65	55.90	4	7	5	5	4	5	2	–1.60	287.22
TPV	–81.21	54.27	2	5	33	2	5	12	4	7.68	602.67
118-D-24	–79.15	52.90	3	6	8	3	4	6	1	1.16	248.22
NVP	–78.28	52.31	1	3	12	4	1	1	4	1.90	266.30
NFV	–78.20	52.26	4	5	31	3	4	12	4	5.36	567.79
AZT	–75.86	50.69	2	6	7	5	4	4	2	–1.91	267.25
LPV	–75.11	50.19	4	5	34	4	5	17	4	5.19	628.81
DRV	–74.39	49.71	3	6	24	3	7	13	4	2.15	546.66
FOS	–72.84	48.68	5	8	24	3	9	15	3	1.50	585.61
ddI	–71.42	47.73	2	5	5	4	3	2	3	0.13	236.23
FTC	–69.28	46.30	2	4	7	3	3	2	2	–0.52	247.25
3TC	–67.57	45.16	2	4	6	3	3	2	2	–0.75	229.26
ddC	–67.24	44.93	2	4	6	3	3	2	2	–0.50	211.22
IDV	–67.07	44.82	4	7	34	5	4	14	5	2.76	613.80
d4T	–66.77	44.62	2	4	7	2	4	2	2	–1.01	224.22
JM-2987	–37.83	25.28	3	3	27	8	0	4	3	0.92	506.83
ATV	–32.48	21.71	5	7	34	6	7	22	3	4.74	704.87
SQV	–27.33	18.27	5	7	34	6	5	16	5	3.31	670.85
RTV	F	-	4	6	36	6	5	22	4	5.00	720.96

Actives range for S_{Dock} indicates the limit above which 95% of the known actives scored. Dark grey indicates compound outside actives range of molecular descriptors

S_{Dock}, docking score using *Chemgauss3* scoring function (FRED software); N_{Dock}, S_{Dock} value normalized to best-scoring known active; a_don, number of hydrogen donors; a_acc, number of hydrogen acceptors; a_hyd, number of hydrophobic atoms; a_nN, number of nitrogens; a_nO, number of oxygens; b_rotN, number of rotatable bonds; rings, number of rings; mw, molar weight (g mol^{-1}); F, compound failed docking test (listed in no specific order). See Table 4 for drug name abbreviations.

ART and the involvement of LXRs, ERs and GR in the regulation of lipid, cholesterol, bone and adipose tissue homeostasis in addition to inflammation, it is plausible that ARVs may also affect these nuclear receptor-signalling pathways. The present study investigated interactions between a large panel of ARV drugs and nuclear receptors LXRα, LXRβ, ERα, ERβ and GR using four different approaches: *in silico* prediction of direct binding to LBDs, cell-free fluorescence co-activator assays to assess direct LBD binding *in vitro*, reporter assays and mRNA expression to detect nuclear receptor-mediated transcriptional activation. These approaches are complementary: the first is theoretically based on the physicochemical properties of the compound and shape of the nuclear receptor binding pocket, and the second is a model system detecting LBD–drug binding but limited to the choice of experimental co-activator, while the third and fourth are biological, taking into account all signalling pathways and not limited to either the LBD or specific co-regulators.

In our study, darunavir and tipranavir (PIs) were predicted ligands of LXRα and LXRβ *in silico*. *In vitro*, both drugs increase PGC1α co-activator recruitment for LXRα and transcriptional activity of at least one of the two receptor isotypes. Additional predicted LXR ligands were the CCR5 receptor antagonists maraviroc and TAK-779, as well as flavopiridol, an anti-cancer agent that has also been reported to inhibit HIV-1 replication *in vitro* (Chao *et al.*, 2000). Maraviroc augmented PGC1α recruitment by LXRα, and although the increase in LXRα transcriptional activity was not significant, the increase in

Table 7

ERα docking score results

			ERα								
Molecule	**S_{Dock}**	**N_{Dock}**	**a_don**	**a_acc**	**a_hyd**	**a_nN**	**a_nO**	**b_rotN**	**rings**	**log P**	**Mw**
Actives range	*<–75.00*		*<4*	*<6*	*10–25*	*<2*	*<6*	*<6*	*<5*	*<6*	*200–375*
AZT	–84.12	79.11	2	6	7	5	4	4	2	–1.91	267.25
FLAV	–80.55	75.76	3	4	21	1	5	2	4	2.90	402.85
TFV	–80.13	75.36	4	7	5	5	4	5	2	–1.60	287.22
118-D-24	–79.16	74.44	3	6	8	3	4	6	1	1.16	248.22
TMC125	–72.89	68.55	2	4	16	6	1	6	3	3.81	435.29
EFV	–72.73	68.40	1	1	17	1	2	3	3	4.10	315.68
d4T	–71.58	67.32	2	4	7	2	4	2	2	–1.01	224.22
MVC	–71.50	67.24	1	4	28	5	1	9	5	6.64	513.68
ddI	–70.11	65.94	2	5	5	4	3	2	3	0.13	236.23
NVP	–69.32	65.19	1	3	12	4	1	1	4	1.90	266.30
FTC	–64.09	60.28	2	4	7	3	3	2	2	–0.52	247.25
3TC	–63.11	59.35	2	4	6	3	3	2	2	–0.75	229.26
ddC	–62.27	58.56	2	4	6	3	3	2	2	–0.50	211.22
ABC	–61.25	57.60	3	4	10	6	1	4	4	0.41	286.34
ATV	F	-	5	7	34	6	7	22	3	4.74	704.87
DRV	F	-	3	6	24	3	7	13	4	2.15	546.66
FOS	F	-	5	8	24	3	9	15	3	1.50	585.61
IDV	F	-	4	7	34	5	4	14	5	2.76	613.80
LPV	F	-	4	5	34	4	5	17	4	5.19	628.81
NFV	F	-	4	5	31	3	4	12	4	5.36	567.79
RTV	F	-	4	6	36	6	5	22	4	5.00	720.96
SQV	F	-	5	7	34	6	5	16	5	3.31	670.85
TPV	F	-	2	5	33	2	5	12	4	7.68	602.67
TAK-779	F	-	1	2	32	2	2	7	5	6.45	495.69
JM-2987	F	-	3	3	27	8	0	4	3	0.92	506.83
RAL	F	-	3	7	15	6	5	8	3	0.81	444.42

Actives range for S_{Dock} indicates the limit above which 95% of the known actives scored. Dark grey indicates compound outside actives range of molecular descriptors

S_{Dock}, docking score using *Chemgauss3* scoring function (FRED software); N_{Dock}, S_{Dock} value normalized to best-scoring known active; a_don, number of hydrogen donors; a_acc, number of hydrogen acceptors; a_hyd, number of hydrophobic atoms; a_nN, number of nitrogens; a_nO, number of oxygens; b_rotN, number of rotatable bonds; rings, number of rings; mw, molar weight (g mol^{-1}); F, compound failed docking test (listed in no specific order). See Table 4 for drug name abbreviations.

LXRβ transcriptional activity was. TAK-779 and flavopiridol both displayed LXRα-antagonistic effects in co-activator assays, and flavopiridol additionally reduced LXRβ transcriptional activity in reporter assays.

Efavirenz, predicted to be a ligand of all five nuclear receptors, had multiple effects: it reduced basal activation of LXRα and LXRβ and increased ERα activation in reporter assays. These findings were confirmed by assessment of ER and LXR target gene expression after exposure to efavirenz. The suppression of LXR activity is supported by reports of reduced expression of LXR target genes *SREBP-1c* (El *et al.*, 2004) and *PPAR-γ* (Gallego-Escuredo *et al.*, 2010) after efavirenz exposure. This is of interest given that efavirenz treatment is associated with depression, anxiety and impaired neurocognition (Lochet *et al.*, 2003), which may reflect inhibition of the neuroprotective effect of LXR activation (Vaya and Schipper, 2007), and ER modulation of monoamine levels in female rat brains (Lubbers *et al.*, 2010). Moreover, ERα-selective activation results in anxiogenic responses in female rats, while ERβ-selective activation is anxiolytic (Lund *et al.*, 2005). Interestingly, activation of ERα by efavirenz could explain why some patients treated with efavirenz develop gynaecomastia (Rahim *et al.*, 2004). In a case study from 2002 (Kegg and Lau, 2002), gynaecomastia in an ART-treated patient was successfully treated with the ER antagonist tamoxifen. This is further supported by a recent publication (Sikora *et al.*, 2010) showing direct efavirenz–ERα binding by competitive binding FRET.

Table 8

ERβ docking score results

			ERβ								
Molecule	**S_{Dock}**	**N_{Dock}**	**a_acc**	**a_don**	**a_hyd**	**a_nN**	**a_nO**	**b_rotN**	**rings**	**logP**	**Mw**
Actives range	*<-70.00*		*<4*	*<6*	*10–25*	*<2*	*<6*	*<6*	*<5*	*<6*	*200–375*
AZT	-77.63	80.09	6	2	7	5	4	4	2	–1.91	267.25
118-D-24	-77.21	79.66	6	3	8	3	4	6	1	1.16	248.22
TFV	-73.19	75.52	7	4	5	5	4	5	2	–1.60	287.22
FLAV	-72.44	74.74	4	3	21	1	5	2	4	2.90	402.85
d4T	-69.59	71.80	4	2	7	2	4	2	2	–1.01	224.22
NVP	-69.28	71.48	3	1	12	4	1	1	4	1.90	266.30
TMC125	-64.62	66.67	4	2	16	6	1	6	3	3.81	435.29
EFV	-64.20	66.23	1	1	17	1	2	3	3	4.10	315.68
FTC	-62.50	64.49	4	2	7	3	3	2	2	–0.52	247.25
ddI	-60.06	61.97	5	2	5	4	3	2	3	0.13	236.23
ddC	-57.74	59.57	4	2	6	3	3	2	2	–0.50	211.22
ABC	-57.56	59.39	4	3	10	6	1	4	4	0.41	286.34
3TC	-57.14	58.96	4	2	6	3	3	2	2	–0.75	229.26
RAL	2.41	-2.49	7	3	15	6	5	8	3	0.81	444.42
JM2987	9.28	-9.57	3	3	27	8	0	4	3	0.92	506.83
ATV	F	-	5	7	34	6	7	22	3	4.74	704.87
DRV	F	-	3	6	24	3	7	13	4	2.15	546.66
FOS	F	-	5	8	24	3	9	15	3	1.50	585.61
IDV	F	-	4	7	34	5	4	14	5	2.76	613.80
LPV	F	-	4	5	34	4	5	17	4	5.19	628.81
NFV	F	-	4	5	31	3	4	12	4	5.36	567.79
RTV	F	-	4	6	36	6	5	22	4	5.00	720.96
SQV	F	-	5	7	34	6	5	16	5	3.31	670.85
TPV	F	-	2	5	33	2	5	12	4	7.68	602.67
MVC	F	-	1	4	28	5	1	9	5	6.64	513.68
TAK-779	F	-	1	2	32	2	2	7	5	6.45	495.69

Actives range for S_{Dock} indicates the limit above which 95% of the known actives scored. Dark grey indicates compound outside actives range of molecular descriptors

S_{Dock}, docking score using *Chemgauss3* scoring function (FRED software); N_{Dock}, S_{Dock} value normalized to best-scoring known active; a_don, number of hydrogen donors; a_acc, number of hydrogen acceptors; a_hyd, number of hydrophobic atoms; a_nN, number of nitrogens; a_nO, number of oxygens; b_rotN, number of rotatable bonds; rings, number of rings; mw, molar weight (g mol^{-1}); F, compound failed docking test (listed in no specific order). See Table 4 for drug name abbreviations.

Although *in silico* predictions and *in vitro* results corresponded well in general, there were some discrepancies. Atazanavir and ritonavir activated LXRα and LXRβ in reporter assays despite being deemed unlikely to fit the respective ligand-binding pockets. In TR-FRET assays no direct binding to LXRα-LBD was detected, which is consistent with data from a previous study showing that ritonavir is not an LXRα-LBD or ERα-LBD ligand (Dussault *et al.*, 2001). In addition, we found that atazanavir did not alter *ABCA1* mRNA expression, while ritonavir inhibited its expression. This is likely to reflect the ability of ritonavir to interact with other nuclear receptors present in the SH-SY5Y cells; for example, PXR can down-regulate ABCA1 expression (Sporstol *et al.*, 2005), and several PIs, including atazanavir and ritonavir, are well-known inducers of PXR (Svard *et al.*, 2010). Alternatively, the effects of atazanavir and ritonavir on LXR reporter activity may be due to allosteric effects. Likewise, an allosteric mechanism may explain the ERα-inductive effect of tipranavir in reporter assays and real-time PCR, as interaction with the ERα-LBD was neither predicted *in silico* nor observed in TR-FRET assays. In contrast, while efavirenz was regarded as a suitable ERα ligand based on docking score and drug structure, and increased ERα activity more than 10-fold in reporter assays, direct binding was not supported by TR-FRET results. This could indicate involvement of other co-factors present in the cell-based reporter assay but not in the cell-free TR-FRET experiments. For example, the steroid receptor co-activator 1 (SRC-1) is expressed in HepG2 cells (Martinez-Jimenez *et al.*,

Table 9

GR docking score results

			GR								
Molecule	**S_{Dock}**	**N_{Dock}**	**a_don**	**a_acc**	**a_hyd**	**a_nN**	**a_nO**	**b_rotN**	**rings**	**log P**	**mw**
Actives range	*<–64.00*		*<3*	*<5*	*15–30*	*<2*	*<5*	*<6*	*<5*	*<8*	*250–500*
FLAV	–90.85	66.14	3	4	21	1	5	2	4	2.90	402.85
EFV	–89.75	64.74	1	1	17	1	2	3	3	4.10	315.68
TFV	–86.07	62.67	4	7	5	5	4	5	2	–1.60	287.22
AZT	–85.04	62.43	2	6	7	5	4	4	2	–1.91	267.25
118-D-24	–84.72	62.40	3	6	8	3	4	6	1	1.16	248.22
ABC	–82.78	59.46	3	4	10	6	1	4	4	0.41	286.34
d4T	–76.27	55.97	2	4	7	2	4	2	2	–1.01	224.22
ddI	–73.84	53.26	2	5	5	4	3	2	3	0.13	236.23
NVP	–72.28	52.51	1	3	12	4	1	1	4	1.90	266.30
TMC125	–71.26	52.09	2	4	16	6	1	6	3	3.81	435.29
FTC	–67.92	48.74	2	4	7	3	3	2	2	–0.52	247.25
3TC	–66.14	47.90	2	4	6	3	3	2	2	–0.75	229.26
ddC	–65.00	47.06	2	4	6	3	3	2	2	–0.50	211.22
RAL	–63.86	33.87	3	7	15	6	5	8	3	0.81	444.42
JM2987	–45.95	32.20	3	3	27	8	0	4	3	0.92	506.83
DRV	–43.69	25.56	3	6	24	3	7	13	4	2.15	546.66
MVC	–34.69	20.66	1	4	28	5	1	9	5	6.64	513.68
FOS	–28.04	13.81	5	8	24	3	9	15	3	1.50	585.61
TPV	–18.74	9.10	2	5	33	2	5	12	4	7.68	602.67
NFV	–12.35	0.00	4	5	31	3	4	12	4	5.36	567.79
ATV	F	-	5	7	34	6	7	22	3	4.74	704.87
IDV	F	-	4	7	34	5	4	14	5	2.76	613.80
LPV	F	-	4	5	34	4	5	17	4	5.19	628.81
RTV	F	-	4	6	36	6	5	22	4	5.00	720.96
SQV	F	-	5	7	34	6	5	16	5	3.31	670.85
TAK-779	F	-	1	2	32	2	2	7	5	6.45	495.69

Actives range for S_{Dock} indicates the limit above which 95% of the known actives scored. Dark grey indicates compound outside actives range of molecular descriptors

S_{Dock}, docking score using *Chemgauss3* scoring function (FRED software); N_{Dock}, S_{Dock} value normalized to best-scoring known active; a_don, number of hydrogen donors; a_acc, number of hydrogen acceptors; a_hyd, number of hydrophobic atoms; a_nN, number of nitrogens; a_nO, number of oxygens; b_rotN, number of rotatable bonds; rings, number of rings; mw, molar weight (g mol^{-1}); F, compound failed docking test (listed in no specific order). See Table 4 for drug name abbreviations.

2006) and has been linked to stimulation of ERα transactivity (Zhou *et al.*, 1998); recruitment of this co-activator by ERα was not investigated in this study.

Tipranavir being identified as an ERα agonist is of interest in light of reported cases of intracranial haemorrhage in patients treated with this PI, causing the FDA to issue a warning in 2006. *In vivo* and *in vitro* investigations revealed decreased platelet aggregation as well as thromboxane B_2 formation following tipranavir treatment (Graff *et al.*, 2008). Coincidentally, oestradiol also reduced production of thromboxane B_2 (Stewart *et al.*, 1999) and inhibited platelet aggregation (Arnal *et al.*, 2006).

Another interesting finding in the present study is LXR activation by atazanavir, darunavir and ritonavir observed in reporter assays. Published *in vitro* experiments exposing mouse skeletal muscle cells to atazanavir, darunavir and lopinavir in combination with ritonavir resulted in increased expression of the LXR target gene *SREBP-1* (Richmond *et al.*, 2010), a transcription factor involved in the regulation of lipid homeostasis. In addition, atazanavir and ritonavir both increased levels of SREBP-1 protein in rat primary hepatocytes (Zhou *et al.*, 2006a). Treatment with ritonavir has a recognized association with hypertriglyceridaemia, a typical effect of LXR-inducing compounds (Schultz *et al.*, 2000). Clinically, the finding that atazanavir and darunavir act as LXR agonists is surprising, as these more recently developed PIs are generally associated with favourable lipid profiles. However, in healthy volunteers treated with ritonavir-boosted atazanavir

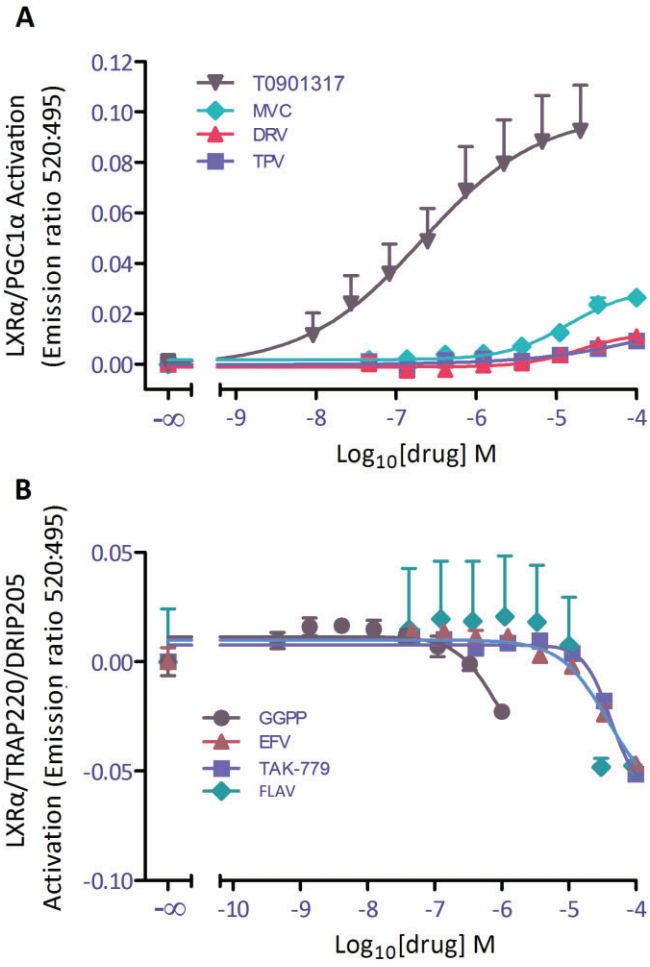

Figure 2

TR-FRET LXRα co-activator assays. A) Validation of LXRα/PGC1α co-activator assay using T0901317, a synthetic LXR agonist. Agonistic effects by maraviroc (MVC), darunavir (DRV) and tipranavir (TPV) on LXRα PGC1α recruitment. B) TR-FRET LXRα co-activator assay, antagonist mode in presence of 1.5 μM T0901317 (LXR agonist, EC_{80}). Known LXR antagonist: geranylgeranyl pyrophosphate (GGPP). Antagonistic effects by efavirenz (EFV), TAK-779 and flavopiridol (FLAV) on LXRα TRAP220/DRIP205 recruitment. Two independent experiments were performed for LXRα assays with triplicate wells ($n = 6$). TR-FRET emission ratio measured after 2 h incubation at room temperature in the dark. Results are presented as means ± S.E.M. IC_{50} values were determined using a sigmoidal dose–response equation in GraphPad Prism version 5.

or darunavir, triglyceride levels are raised (Tomaka *et al.*, 2009). Similarly, lipohypertrophy of the dorso-cervical region of the neck has been reported in a female HIV patient treated with unboosted atazanavir plus raltegravir (Ceccarelli *et al.*, 2011). Moreover, hypertriglyceridaemia can also be generated through a PXR-mediated and SREBP-independent pathway, as occurs in rifampicin-treated mice (Zhou *et al.*, 2006b). This effect may be more dominant than LXR activation, and indeed ritonavir appears to be a more potent inducer of PXR than atazanavir (Gupta *et al.*, 2008). In the present study the disparity between the real-time PCR and reporter assays for some of the ARV agents tested probably reflects the difficulty in distinguishing LXR-mediated from PXR-mediated effects, as discussed previously.

Despite similarities between Cushing's syndrome and ART-associated lipodystrophy, there was no significant effect on GR transcriptional activity by any of the ARV drugs tested in the study. However, pseudo-Cushing's syndrome seen in patients on ART could also be caused by activation of PXR; cases of misdiagnosis have been described in patients receiving rifampicin treatment for tuberculosis (Terzolo *et al.*, 1995), and PXR agonists have been demonstrated to disrupt glucocorticoid homeostasis in transgenic mice (Zhai *et al.*, 2007). Indeed, many ARV drugs are inducers of PXR (Svard *et al.*, 2010).

As HIV disease and its treatment are highly complex, adverse effects of ART are likely to be multifactorial, and it may not be possible to ascribe effects to the activation of a single nuclear receptor. Indeed, there is a significant cross-talk between nuclear receptors, and the activation of one may often have an indirect impact on others. However, identifying direct effects of single ARV drugs on individual nuclear receptors may help explain, at least in part, the underlying mechanisms of ART-associated adverse events. It would be of interest to extend this investigation to include other nuclear receptors, such as vitamin D receptor and farnesoid X receptor, which are also involved in cholesterol and lipid homeostasis, insulin resistance, adipocyte differentiation and bone formation.

In silico computational methods are often used in drug discovery as a means of screening large libraries of compounds and identifying possible receptor ligands, which would not be possible or cost-effective by *in vitro* or biochemical assays. In this study, we utilized molecular modelling in a reverse manner to assess the ability of already approved or investigational antiretroviral drugs to activate nuclear receptors. Furthermore, cell-free LBD-binding experiments, cell-based reporter assays and mRNA target gene expression assays were carried out to identify ligands of LXRα, LXRβ, ERα, ERβ and GR from a library of ARV drugs. We have demonstrated that several ARV drugs have the ability to act as ligands of LXRα, LXRβ and/or ERα. Further investigations to elucidate the downstream effects and clinical relevance of ARV interactions with LXRα, LXRβ and ERα, as well as assessment of ARV binding to other nuclear receptors not investigated in this study, may aid in predicting 'off-target' effects of ART and prove valuable in the development of newer agents to reduce the risk of metabolic abnormalities. Some discrepancies observed between results generated by different methods highlight the value of using complementary approaches and model systems to better understand these interactions.

Acknowledgements

This study was funded by the European AIDS Clinical Society. We thank the software vendors for their continuing support of such academic research efforts, in particular the contributions of Accelrys, the Chemical Computing Group, and OpenEye Scientific. The Trinity Biomedical Sciences Institute is supported by a capital infrastructure investment from Cycle 5 of the Irish Higher Education Authority's Programme

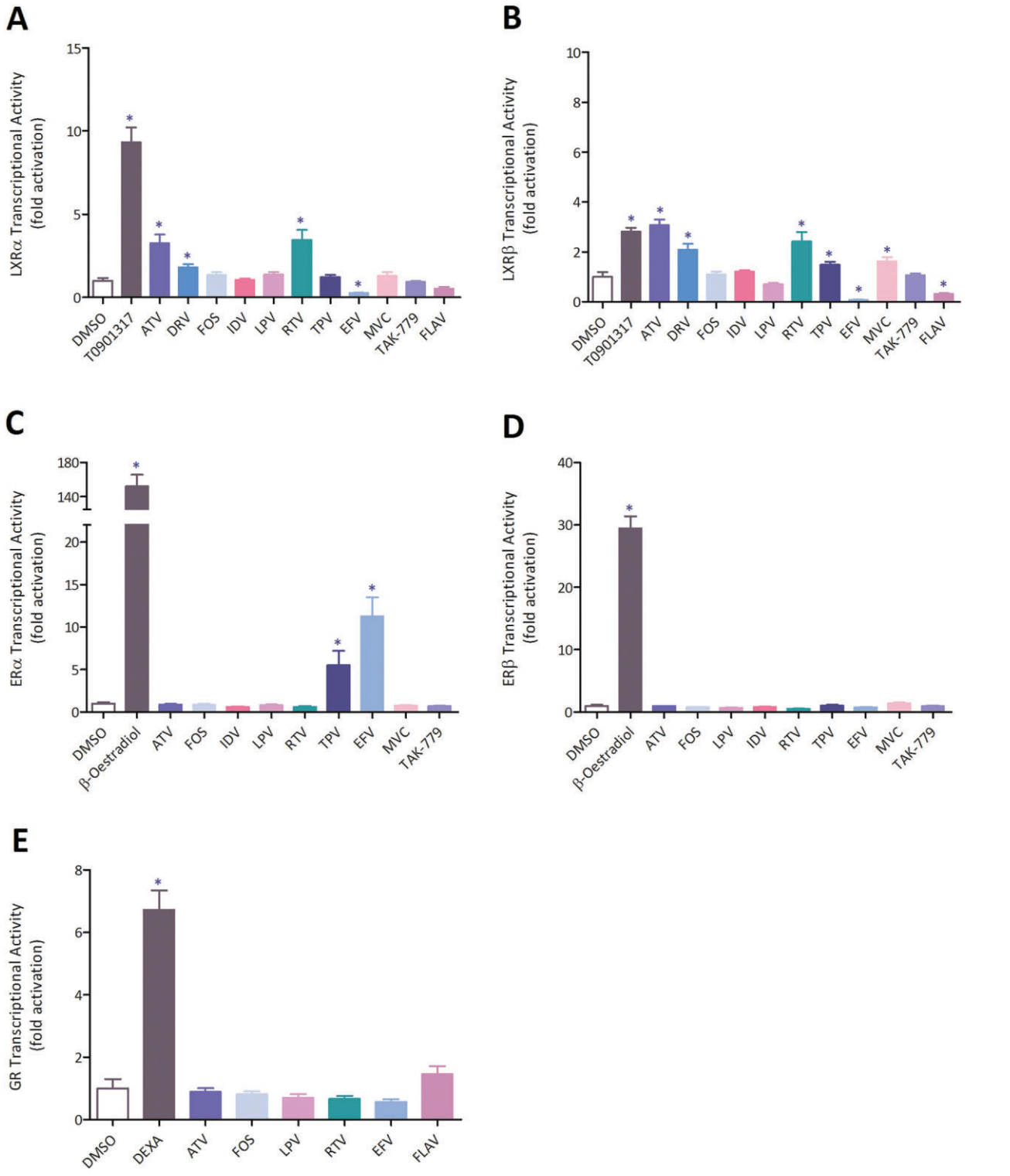

Figure 3

Effect of ARVs on LXR, ER and GR transcriptional activity as measured by Dual-Luciferase Reporter Assays expressed as fold activation relative to vehicle (DMSO) control: A) LXRα, B) LXRβ, C) ERα, D) ERβ and E) GR. HepG2 cells were transfected with nuclear receptor expression plasmids and the corresponding responsive element–luciferase construct. Five independent experiments were performed in duplicates for each treatment. All ARV drugs were used at 10 μM except nelfinavir (NFV, 1 μM) and flavopiridol (FLAV, 100 nM), due to cytotoxicity. Positive controls (LXR: 10 μM T0901317, ER: 100 nM 17β-oestradiol, GR: 1 μM dexamethasone) and a vehicle control (0.1% DMSO) were included. *$P < 0.05$ by one-way ANOVA analysis with Dunnett's *post hoc* analysis. ATV, atazanavir; DEX, dexamethasone; DRV, darunavir; EFV, efavirenz; FLAV, flavopiridol; FOS, fosamprenavir; IDV, indinavir; LPV, lopinavir; MVC, maraviroc; NFV, nelfinavir; RTV, ritonavir; TPV, tipranavir.

Table 10

Summary: assessment of ARV drug-nuclear receptor interactions by *in silico* modelling, TR-FRET and reporter assays

	LXRα				LXRβ				ERα				ERβ		GR	
Drug	**N_{Dock}**	**EC_{50}/IC_{50} (μM)**	**Maximum response[a], %**	**Reporter assay fold change**	**N_{Dock}**	**EC_{50} (nM)**	**Maximum response[a], %**	**Reporter assay fold change**	**N_{Dock}**	**EC_{50} (nM)**	**Maximum response[a], %**	**Reporter assay fold change**	**N_{Dock}**	**Reporter assay fold change**	**N_{Dock}**	**Reporter assay fold change**
GW	100	0.13 (SRC1 LiSA)[d]	–	–	100	30 (hLXRβ-GAL4)[d]	–	–	–	–	–	–	–	–	–	–
T	–	0.21 (PGC1α)	100	9.3 ± 0.9***	–	304 (D22)	–	2.8 ± 0.2	–	–	–	–	–	–	–	–
E2	–	–	–	–	–	–	–	–	100	0.74 (PGC1α)	100	152 ± 13.7***	100	29.4 ± 2.0***	–	–
DEXA	–	–	–	–	–	–	–	–	–	–	–	–	–	–	100	6.7 ± 0.6***
ATV	–	–	NR	3.3 ± 0.5***	*21.71* [c]	–	NR	3.1 ± 0.2***	–	–	NR	0.9 ± 0.1	–	0.9 ± 0.1	–	0.9 ± 0.1
DRV	68.23	19.1 (PGC1α)	11.9***	1.8 ± 0.2*	49.71	–	NR	2.1 ± 0.2***	–	–	–	–	–	–	–	–
FOS	40.41 [c]	–	NR	1.3 ± 0.2	48.68	–	–	1.1 ± 0.1	–	–	NR	0.8 ± 0.1	–	0.8 ± 0.02	13.81[c]	0.8 ± 0.1
IDV	52.61 [c]	–	NR	1.0 ± 0.1	44.82 [c]	–	–	1.2 ± 0.1	–	–	NR	0.6 ± 0.1	–	0.8 ± 0.1	–	–
LPV	2.01 [c]	–	NR	1.4 ± 0.2	50.19 [c]	–	–	0.7 ± 0.1	–	–	NR	0.8 ± 0.1	–	0.7 ± 0.03	–	0.7 ± 0.1
RTV	–	–	NR	3.5 ± 0.6***	–	–	NR	2.4 ± 0.4***	–	–	NR	0.6 ± 0.1	–	0.5 ± 0.1	–	0.7 ± 0.1
TPV	41.28	347.5 (PGC1α)	10.4***	1.2 ± 0.1	54.27	–	NR	1.5 ± 0.1*	–	–	NR	5.5 ± 1.7***	–	1.1 ± 0.1	–	–
EFV	58.57	39.2 (TRAP/DRIP)	64.0***[b]	0.26 ± 0.03***	56.74	–	NR	0.08 ± 0.01***	68.40	–	NR	11.3 ± 2.2***	66.23	0.7 ± 0.1	64.74	0.6 ± 0.1
MVC	66.43	14.5 (PGC1α)	28.9***	1.3 ± 0.2	66.72	–	NR	1.6 ± 0.2**	67.24	–	NR	0.8 ± 0.1	–	1.4 ± 0.2	–	–
TAK–779	42.43	41.7 (TRAP/DRIP)	60.2*** [b]	0.93 ± 0.06	72.09	–	NR	1.1 ± 0.1	–	–	Precipitation	0.7 ± 0.1	–	0.8 ± 0.1	–	–
FLAV	60.01	NC (TRAP/DRIP)	NR [b]	0.52 ± 0.11	59.91	–	NR	0.32 ± 0.04**	–	–	–	–	–	–	66.14	1.5 ± 0.3
GGPP	N.A.	0.79 (TRAP/DRIP)	82.5** [b]	–	–	–	–	–	–	–	–	–	–	–	–	–

*$P < 0.05$; **$P < 0.01$; ***$P < 0.001$ compared with vehicle control.

[a]Maximum response rate compared with 20 μM T0901317 or 1 μM 17β-oestradiol.

[b]Maximum response rate compared with 1.5 μM T0901317 (in LXRα/TRAP220/DRIP205 antagonist assays).

[c]Failed molecular descriptor filter test.

[d]Data from Collins *et al.*, 2002 (SCR1 LiSA = cell-free ligand-sensing assay using SRC1, hLXRβ-GAL4 = cell-based reporter gene assay using a GAL4 reporter).

GW, GW3965 (LXR agonist); T, T0901317; E2, 17β-oestradiol; DEXA, dexamethasone; N_{Dock}, docking score normalized to best scoring known active; NC, not converged; NR, no response at the maximum concentration tested. See Table 4 for other drug name abbreviations.

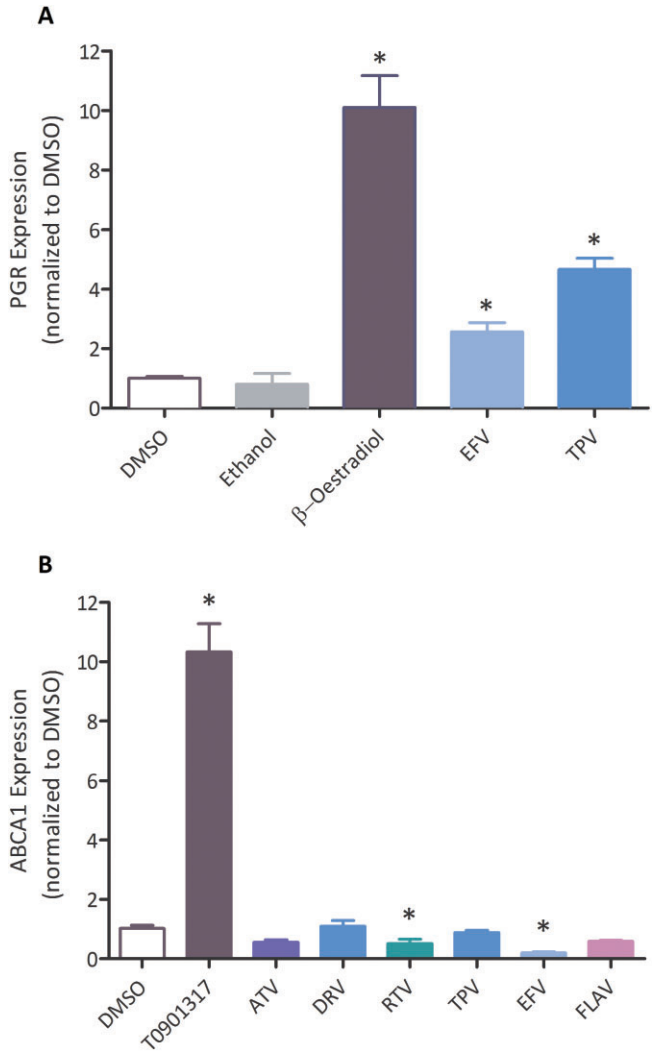

Figure 4

Effect of ARVs on LXR and ER target gene expression as measured by quantitative real-time PCR, normalized to *GAPDH* and expressed as fold activation relative to vehicle (DMSO) control: A) LXR target gene *ABCA1* expression in SH-SY5Y cells; B) ER target gene *PGR* expression in MCF-7 cells. Five independent experiments were performed for each treatment. All ARV drugs were used at 10 μM except flavopiridol (FLAV, 100 nM), due to cytotoxicity. Positive controls (LXR: 10 μM T0901317, ER: 100 nM 17β-oestradiol) and vehicle controls (0.1% DMSO, and additionally 0.1% ethanol for ER) were included. *$P < 0.05$ by one-way ANOVA analysis with Dunnett's *post hoc* analysis. ATV, atazanavir; DRV, darunavir; EFV, efavirenz; FLAV, flavopiridol; RTV, ritonavir; TPV, tipranavir.

for Research in Third Level Institutions (PRTLI). FB thanks the support of the European Commission (Marie Curie grant, People FP7, Project Reference: 274988). Calculations were performed on the Stokes cluster maintained by the Irish Centre for High-End Computing and local infrastructure provided by Dell Ireland and maintained by the Trinity Centre for High Performance Computing. We would like to thank Dr Martin Peters and Paddy Doyle for their assistance.

Conflict of interest

None.

References

Alexander SPH *et al.* (2013). The Concise Guide to PHARMACOLOGY 2013/14: Overview. Br J Pharmacol 170: 1449–1867.

Allred KF, Smart EJ, Wilson ME (2006). Estrogen receptor-alpha mediates gender differences in atherosclerosis induced by HIV protease inhibitors. J Biol Chem 281: 1419–1425.

Arnal JF, Douin-Echinard V, Brouchet L, Tremollieres F, Laurell H, Lenfant F *et al.* (2006). Understanding the oestrogen action in experimental and clinical atherosclerosis. Fundam Clin Pharmacol 20: 539–548.

Bastard JP, Caron M, Vidal H, Jan V, Auclair M, Vigouroux C *et al.* (2002). Association between altered expression of adipogenic factor SREBP1 in lipoatrophic adipose tissue from HIV-1-infected patients and abnormal adipocyte differentiation and insulin resistance. Lancet 359: 1026–1031.

Caron M, Auclair M, Vigouroux C, Glorian M, Forest C, Capeau J (2001). The HIV protease inhibitor indinavir impairs sterol regulatory element-binding protein-1 intranuclear localization, inhibits preadipocyte differentiation, and induces insulin resistance. Diabetes 50: 1378–1388.

Ceccarelli G, D'Ettorre G, Marchetti F, Rizza C, Mastroianni CM, Carlesimo B *et al.* (2011). Development of buffalo hump in the course of antiretroviral therapy including raltegravir and unboosted atazanavir: a case report and review of the literature. J Med Case Rep 5: 70. doi: 10.1186/1752-1947-5-70.

Chao SH, Fujinaga K, Marion JE, Taube R, Sausville EA, Senderowicz AM *et al.* (2000). Flavopiridol inhibits P-TEFb and blocks HIV-1 replication. J Biol Chem 275: 28345–28348.

Collins JL, Fivush AM, Watson MA, Galardi CM, Lewis MC, Moore LB *et al.* (2002). Identification of a nonsteroidal liver X receptor agonist through parallel array synthesis of tertiary amines. J Med Chem 45: 1963–1966.

Dahlman-Wright K, Cavailles V, Fuqua SA, Jordan VC, Katzenellenbogen JA, Korach KS *et al.* (2006). International Union of Pharmacology. LXIV. Estrogen receptors. Pharmacol Rev 58: 773–781.

van den Driesche S, Smith VM, Myers M, Duncan WC (2008). Expression and regulation of oestrogen receptors in the human corpus luteum. Reproduction 135: 509–517.

Dussault I, Lin M, Hollister K, Wang EH, Synold TW, Forman BM (2001). Peptide mimetic HIV protease inhibitors are ligands for the orphan receptor SXR. J Biol Chem 276: 33309–33312.

Ekins S, Mirny L, Schuetz EG (2002). A ligand-based approach to understanding selectivity of nuclear hormone receptors PXR, CAR, FXR, LXRα, and LXRβ. Pharm Res 19: 1788–1800.

El HK, Glorian M, Monsempes C, Dieudonne MN, Pecquery R, Giudicelli Y *et al.* (2004). In vitro suppression of the lipogenic pathway by the nonnucleoside reverse transcriptase inhibitor efavirenz in 3T3 and human preadipocytes or adipocytes. J Biol Chem 279: 15130–15141.

Gallego-Escuredo JM, Del Mar Gutierrez M, Diaz-Delfin J, Domingo JC, Mateo MG, Domingo P *et al.* (2010). Differential effects of efavirenz and lopinavir/ritonavir on human adipocyte differentiation, gene expression and release of adipokines and pro-inflammatory cytokines. Curr HIV Res 8: 545–553.

Graff J, Von HN, Kuczka K, Angioni C, Gute P, Klauke S *et al.* (2008). Significant effects of tipranavir on platelet aggregation and thromboxane B2 formation in vitro and in vivo. J Antimicrob Chemother 61: 394–399.

Gupta A, Mugundu GM, Desai PB, Thummel KE, Unadkat JD (2008). Intestinal human colon adenocarcinoma cell line LS180 is an excellent model to study pregnane X receptor, but not constitutive androstane receptor, mediated CYP3A4 and multidrug resistance transporter 1 induction: studies with anti-human immunodeficiency virus protease inhibitors. Drug Metab Dispos 36: 1172–1180.

Hall JM, McDonnell DP (1999). The estrogen receptor β-isoform (ERβ) of the human estrogen receptor modulates ERα transcriptional activity and is a key regulator of the cellular response to estrogens and antiestrogens. Endocrinology 140: 5566–5578.

Haugaard SB (2006). Toxic metabolic syndrome associated with HAART. Expert Opin Drug Metab Toxicol 2: 429–445.

Hawkins PC, Skillman AG, Warren GL, Ellingson BA, Stahl MT (2010). Conformer generation with OMEGA: algorithm and validation using high quality structures from the Protein Databank and Cambridge Structural Database. J Chem Inf Model 50: 572–584.

Huang N, Shoichet BK, Irwin JJ (2006). Benchmarking sets for molecular docking. J Med Chem 49: 6789–6801.

Kegg S, Lau R (2002). Tamoxifen in antiretroviral-associated gynaecomastia. Int J STD AIDS 13: 582–583.

Krasowski MD, Ni A, Hagey LR, Ekins S (2011). Evolution of promiscuous nuclear hormone receptors: LXR, FXR, VDR, PXR, and CAR. Mol Cell Endocrinol 334: 39–48.

Kratz M, Purnell JQ, Breen PA, Thomas KK, Utzschneider KM, Carr DB *et al.* (2008). Reduced adipogenic gene expression in thigh adipose tissue precedes human immunodeficiency virus-associated lipoatrophy. J Clin Endocrinol Metab 93: 959–966.

Lochet P, Peyriere H, Lotthe A, Mauboussin JM, Delmas B, Reynes J (2003). Long-term assessment of neuropsychiatric adverse reactions associated with efavirenz. HIV Med 4: 62–66.

Lu NZ, Wardell SE, Burnstein KL, Defranco D, Fuller PJ, Giguere V *et al.* (2006). International Union of Pharmacology. LXV. The pharmacology and classification of the nuclear receptor superfamily: glucocorticoid, mineralocorticoid, progesterone, and androgen receptors. Pharmacol Rev 58: 782–797.

Lubbers LS, Zafian PT, Gautreaux C, Gordon M, Alves SE, Correa L *et al.* (2010). Estrogen receptor (ER) subtype agonists alter monoamine levels in the female rat brain. J Steroid Biochem Mol Biol 122: 310–317.

Lund TD, Rovis T, Chung WC, Handa RJ (2005). Novel actions of estrogen receptor-beta on anxiety-related behaviors. Endocrinology 146: 797–807.

Martinez-Jimenez CP, Castell JV, Gomez-Lechon MJ, Jover R (2006). Transcriptional activation of CYP2C9, CYP1A1, and CYP1A2 by hepatocyte nuclear factor 4α requires coactivators peroxisomal proliferator activated receptor-gamma coactivator 1α and steroid receptor coactivator 1. Mol Pharmacol 70: 1681–1692.

Nguyen AT, Gagnon A, Angel JB, Sorisky A (2000). Ritonavir increases the level of active ADD-1/SREBP-1 protein during adipogenesis. AIDS 14: 2467–2473.

Oberkofler H, Schraml E, Krempler F, Patsch W (2003). Potentiation of liver X receptor transcriptional activity by peroxisome-proliferator-activated receptor gamma co-activator 1 alpha. Biochem J 371: 89–96.

Onnis V, Kinsella GK, Carta G, Jagoe WN, Price T, Williams DC *et al.* (2010). Virtual screening for the identification of novel nonsteroidal glucocorticoid modulators. J Med Chem 53: 3065–3074.

Pfaffl MW (2001). A new mathematical model for relative quantification in real-time RT-PCR. Nucleic Acids Res 29: e45.

Rahim S, Ortiz O, Maslow M, Holzman R (2004). A case–control study of gynecomastia in HIV-1-infected patients receiving HAART. AIDS Read 14: 23–32, 35.

Repa JJ, Liang G, Ou J, Bashmakov Y, Lobaccaro JM, Shimomura I *et al.* (2000). Regulation of mouse sterol regulatory element-binding protein-1c gene (SREBP-1c) by oxysterol receptors, LXRα and LXRβ. Genes Dev 14: 2819–2830.

Richmond SR, Carper MJ, Lei X, Zhang S, Yarasheski KE, Ramanadham S (2010). HIV-protease inhibitors suppress skeletal muscle fatty acid oxidation by reducing CD36 and CPT1 fatty acid transporters. Biochim Biophys Acta 1801: 559–566.

Riddle TM, Kuhel DG, Woollett LA, Fichtenbaum CJ, Hui DY (2001). HIV protease inhibitor induces fatty acid and sterol biosynthesis in liver and adipose tissues due to the accumulation of activated sterol regulatory element-binding proteins in the nucleus. J Biol Chem 276: 37514–37519.

Schultz JR, Tu H, Luk A, Repa JJ, Medina JC, Li L *et al.* (2000). Role of LXRs in control of lipogenesis. Genes Dev 14: 2831–2838.

Seo JB, Moon HM, Kim WS, Lee YS, Jeong HW, Yoo EJ *et al.* (2004). Activated liver X receptors stimulate adipocyte differentiation through induction of peroxisome proliferator-activated receptor gamma expression. Mol Cell Biol 24: 3430–3444.

Sikora MJ, Rae JM, Johnson MD, Desta Z (2010). Efavirenz directly modulates the oestrogen receptor and induces breast cancer cell growth. HIV Med 11: 603–607.

Son YL, Lee YC (2009). Molecular determinants of the interactions between LXR/RXR heterodimers and TRAP220. Biochem Biophys Res Commun 384: 389–393.

Sporstol M, Tapia G, Malerod L, Mousavi SA, Berg T (2005). Pregnane X receptor-agonists down-regulate hepatic ATP-binding cassette transporter A1 and scavenger receptor class B type I. Biochem Biophys Res Commun 331: 1533–1541.

Stafslien DK, Vedvik KL, De Rosier T, Ozers MS (2007). Analysis of ligand-dependent recruitment of coactivator peptides to RXRβ in a time-resolved fluorescence resonance energy transfer assay. Mol Cell Endocrinol 264: 82–89.

Stewart KG, Zhang Y, Davidge ST (1999). Estrogen decreases prostaglandin H synthase products from endothelial cells. J Soc Gynecol Investig 6: 322–327.

Stulnig TM, Oppermann U, Steffensen KR, Schuster GU, Gustafsson JA (2002). Liver X receptors downregulate 11β-hydroxysteroid dehydrogenase type 1 expression and activity. Diabetes 51: 2426–2433.

Sutinen J, Kannisto K, Korsheninnikova E, Nyman T, Ehrenborg E, Andrew R *et al.* (2004). In the lipodystrophy associated with highly active antiretroviral therapy, pseudo-Cushing's syndrome is associated with increased regeneration of cortisol by 11β-hydroxysteroid dehydrogenase type 1 in adipose tissue. Diabetologia 47: 1668–1671.

Svard J, Spiers JP, Mulcahy F, Hennessy M (2010). Nuclear receptor-mediated induction of CYP450 by antiretrovirals: functional consequences of NR1I2 (PXR) polymorphisms and differential prevalence in Whites and Sub-Saharan Africans. J Acquir Immune Defic Syndr 55: 536–549.

Tcherepanova I, Puigserver P, Norris JD, Spiegelman BM, McDonnell DP (2000). Modulation of estrogen receptor-alpha transcriptional activity by the coactivator PGC-1. J Biol Chem 275: 16302–16308.

Terzolo M, Borretta G, Ali A, Cesario F, Magro G, Boccuzzi A *et al*. (1995). Misdiagnosis of Cushing's syndrome in a patient receiving rifampicin therapy for tuberculosis. Horm Metab Res 27: 148–150.

Tomaka F, Lefebvre E, Sekar V, Van BB, Vangeneugden T, Vandevoorde A *et al*. (2009). Effects of ritonavir-boosted darunavir vs. ritonavir-boosted atazanavir on lipid and glucose parameters in HIV-negative, healthy volunteers. HIV Med 10: 318–327.

Vaya J, Schipper HM (2007). Oxysterols, cholesterol homeostasis, and Alzheimer disease. J Neurochem 102: 1727–1737.

Vega RB, Huss JM, Kelly DP (2000). The coactivator PGC-1 cooperates with peroxisome proliferator-activated receptor alpha in transcriptional control of nuclear genes encoding mitochondrial fatty acid oxidation enzymes. Mol Cell Biol 20: 1868–1876.

Wong J, Quinn CM, Brown AJ (2007). Synthesis of the oxysterol, 24(*S*),25-epoxycholesterol, parallels cholesterol production and may protect against cellular accumulation of newly-synthesized cholesterol. Lipids Health Dis 6: 10. doi: 10.1186/1476-511X-6-10.

Yang Z, Guo C, Zhu P, Li W, Myatt L, Sun K (2007). Role of glucocorticoid receptor and CCAAT/enhancer-binding protein α in the feed-forward induction of 11β-hydroxysteroid dehydrogenase type 1 expression by cortisol in human amnion fibroblasts. J Endocrinol 195: 241–253.

Zhai Y, Pai HV, Zhou J, Amico JA, Vollmer RR, Xie W (2007). Activation of pregnane X receptor disrupts glucocorticoid and mineralocorticoid homeostasis. Mol Endocrinol 21: 138–147.

Zhou G, Cummings R, Li Y, Mitra S, Wilkinson HA, Elbrecht A *et al*. (1998). Nuclear receptors have distinct affinities for coactivators: characterization by fluorescence resonance energy transfer. Mol Endocrinol 12: 1594–1604.

Zhou H, Pandak WM Jr, Lyall V, Natarajan R, Hylemon PB (2005). HIV protease inhibitors activate the unfolded protein response in macrophages: implication for atherosclerosis and cardiovascular disease. Mol Pharmacol 68: 690–700.

Zhou H, Gurley EC, Jarujaron S, Ding H, Fang Y, Xu Z *et al*. (2006a). HIV protease inhibitors activate the unfolded protein response and disrupt lipid metabolism in primary hepatocytes. Am J Physiol Gastrointest Liver Physiol 291: G1071–G1080.

Zhou J, Zhai Y, Mu Y, Gong H, Uppal H, Toma D *et al*. (2006b). A novel pregnane X receptor-mediated and sterol regulatory element-binding protein-independent lipogenic pathway. J Biol Chem 281: 15013–15020.